



**POLITECNICO**  
MILANO 1863

SCUOLA DI INGEGNERIA INDUSTRIALE  
E DELL'INFORMAZIONE

EXECUTIVE SUMMARY OF THE THESIS

# High Order Efficient Station Keeping Strategy for Low-Thrust Geostationary Satellites with Differential Algebra Techniques

LAUREA MAGISTRALE IN SPACE ENGINEERING - INGEGNERIA SPAZIALE

**Author:** STEFANO CARCANO

**Advisor:** PROF. PIERLUIGI DI LIZIA

**Co-advisor:** MICHELE MAESTRINI

**Academic year:** 2021-2022

## 1. Introduction

Due to the high number of active satellites placed on the Geostationary Earth Orbit (GEO), it is necessary to guarantee their cohabitation and prevent any possible collision. A longitude and latitude drift from the desired coordinates is expected to occur because of the presence of constant perturbations, generated by the non spherical Earth gravitational field, and time-variant ones, such as the soli-lunar attraction and the solar radiation pressure (SRP) acting on the body. An active control is then mandatory to maintain the spacecraft in its assigned slot, made of stringent angular bands permitting only contained displacements (typically less than  $0.1^\circ$ ) around the nominal location. This set of programmed actions is called Station Keeping (SK) strategy. It is nowadays achieved by exploiting low-thrust electric engines, optimizing the thrust arcs and the whole sequence of firings. It is therefore possible to save propellant mass while consequently increasing the payload one and the mission lifetime. Real SK problems are usually faced through linear approximations of the dynamics as in [5], or thanks to heavy numerical algorithms, as done by [1], including thrusters configuration and constraints

on the duration of the firings. Already explored by [4], high order control allows to tackle the high nonlinearities, to reach a more optimized, accurate solution than linear ones and to reduce the computational burden required by the classical numerical methods. This can be obtained exploiting Differential Algebra (DA) techniques to solve a feedback optimal control problem (OCP) with mere evaluations of polynomial maps. This thesis proposes a new, possible approach to geostationary SK, proving the potential of DA in this particular field, by considering a preliminary and simplified simulation, including unbounded thrust, no particular engines layout and the absence of path constraints during the powered phases. The workflow foresees a target determination procedure, followed by the solution of both an Energy Optimal Problem (EOP) and a Fuel Optimal one (FOP).

## 2. Fundamentals

### 2.1. Free-Drift Dynamics

Affected by the geopotential perturbation, the Sun and Moon influence and the SRP, when a GEO satellite is free to naturally drift from its assigned location ( $[l_s, 0^\circ]$ ), its dynamics can be

described by a perturbed ( $\mathbf{a}_p$ ) Two-Body Problem (TBP) as in Equation 1:

$$\ddot{\mathbf{r}} = -\frac{\mu}{r^3} \mathbf{r} + \mathbf{a}_p \quad (1)$$

This motion can be turned and integrated in the Earth Centered Earth Fixed (ECEF, Figure 1) spherical coordinates  $r$ ,  $\lambda$  and  $\phi$ : distance, longitude and latitude respectively.

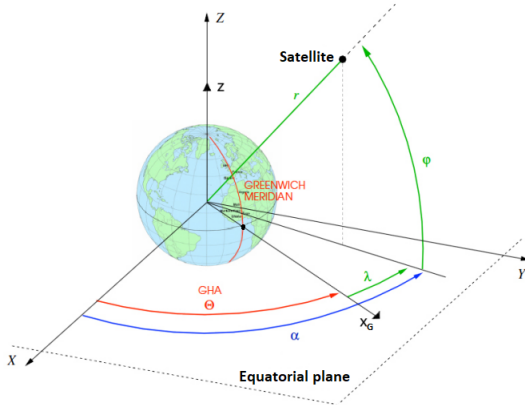


Figure 1: *ECEF Reference Frame.*  $X, Y, Z$ : Geocentric Equatorial Reference System;  $\Theta$ : Greenwich Hour Angle;  $\alpha$ : Right Ascension

As a consequence, a latitude displacement of  $0.85^\circ/\text{year}$  occurs, as well as a longitude one, whose magnitude depends on the nominal coordinate. For a spacecraft located at  $60^\circ E$ , the longitude drift rate is about  $30^\circ/\text{year}$ .

## 2.2. High Order Feedback SK OCP

In order to counteract these disturbances, a set of manoeuvres shall be scheduled to ensure that the satellite won't violate the slot bounds shown in Figure 2 ( $\lambda_{max}$ ,  $\phi_{max}$ ).

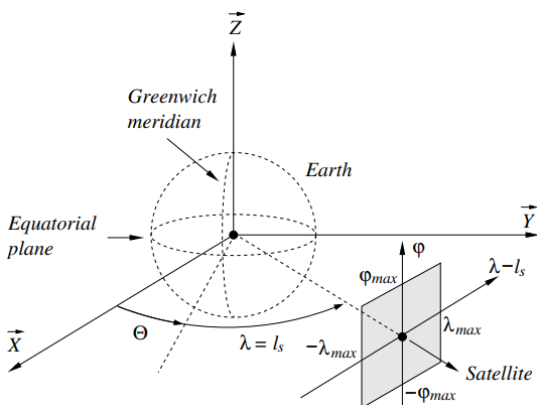


Figure 2: *Station Keeping Window in ECEF frame*

These low-thrust phases generate a sequence of controlled trajectories. Each one can be optimized with the aim of minimizing a certain cost function. Introducing the state ( $\mathbf{x}$ ) and costate ( $\mathbf{l}$ ) formulation and their dynamical flows  $f, g$ , thanks to the calculus of variations, the considered, generic OCP can be transformed into a Two-Point Boundary Value Problem (TPBVP):

$$\begin{cases} \dot{\mathbf{x}} = f(\mathbf{x}, \mathbf{l}, t) \\ \dot{\mathbf{l}} = g(\mathbf{x}, \mathbf{l}, t) \end{cases} \quad (2)$$

subject to initial and final conditions on the state  $\mathbf{x}$ . Thanks to DA, an arbitrary order  $k$  Taylor series expansion of the solution of the TPBVP with respect to initial and final state can be performed in a computer environment. The first step consists in initializing the state and the costate at initial time as DA variables about a reference  $\bar{\mathbf{x}}_0, \bar{\mathbf{l}}_0$ :

$$\mathbf{x}_0 = \bar{\mathbf{x}}_0 + \delta\mathbf{x}_0 \quad (3a)$$

$$\mathbf{l}_0 = \bar{\mathbf{l}}_0 + \delta\mathbf{l}_0 \quad (3b)$$

The dependence of the final conditions on the initial state and costate values is obtained in terms of high order polynomial maps ( $M$ ). Using the DA expansion techniques, the solution at final time is expressed as a  $k$  order polynomial with respect to the starting conditions, as in [2].

$$\begin{pmatrix} [\mathbf{x}_f] \\ [\mathbf{l}_f] \end{pmatrix} = \begin{pmatrix} \bar{\mathbf{x}}_f + \delta\mathbf{x}_f \\ \bar{\mathbf{l}}_f + \delta\mathbf{l}_f \end{pmatrix} = \begin{pmatrix} M_{\mathbf{x}_f} \\ M_{\mathbf{l}_f} \end{pmatrix} \begin{pmatrix} \delta\mathbf{x}_0 \\ \delta\mathbf{l}_0 \end{pmatrix} \quad (4)$$

Subtracting the constant parts:

$$\begin{pmatrix} \delta\mathbf{x}_f \\ \delta\mathbf{l}_f \end{pmatrix} = \begin{pmatrix} M_{\mathbf{x}_f} \\ M_{\mathbf{l}_f} \end{pmatrix} \begin{pmatrix} \delta\mathbf{x}_0 \\ \delta\mathbf{l}_0 \end{pmatrix} \quad (5)$$

and extracting the map for the final state, the following new relation can be built concatenating  $M_{\mathbf{x}_f}$  with the identity map  $I_{\mathbf{x}_0}$  related to the initial state variation:

$$\begin{pmatrix} \delta\mathbf{x}_f \\ \delta\mathbf{x}_0 \end{pmatrix} = \begin{pmatrix} M_{\mathbf{x}_f} \\ I_{\mathbf{x}_0} \end{pmatrix} \begin{pmatrix} \delta\mathbf{x}_0 \\ \delta\mathbf{l}_0 \end{pmatrix} \quad (6)$$

By virtue of the polynomial inversion techniques:

$$\begin{pmatrix} \delta\mathbf{x}_0 \\ \delta\mathbf{l}_0 \end{pmatrix} = \begin{pmatrix} M_{\mathbf{x}_f} \\ I_{\mathbf{x}_0} \end{pmatrix}^{-1} \begin{pmatrix} \delta\mathbf{x}_f \\ \delta\mathbf{x}_0 \end{pmatrix} \quad (7)$$

the initial costate displacement with respect to the reference, representing the optimal control law, can be finally found imposing a desired  $\delta\mathbf{x}_f$ :

$$\begin{aligned} \delta\mathbf{l}_0 &= M_{\mathbf{l}_0}(\delta\mathbf{x}_f, \delta\mathbf{x}_0) \\ \mathbf{l}_0 &= \bar{\mathbf{l}}_0 + \delta\mathbf{l}_0 \end{aligned} \quad (8)$$

### 3. Methodology

The SK strategy adopted in this thesis is based on a cyclic sequence made of a free-drift (FD) stage followed by a controlled section targeting a specific point inside the allowable region, tailored to maximize the free permanence within the permitted latitude-longitude bands until the next powered phase starts. A year evolution is considered for the test spacecraft in Table 1 and from January 1<sup>st</sup>, 2023 at 00 : 00. DA is applied to compute the optimal, arbitrary order solution for each one-day long fixed thrust arc. Thanks to this, 14 control cycles in a year are needed. Due to the time dependence of the disturbances, each target is different, as well as the duration of each FD track, as shown in Figure 3.

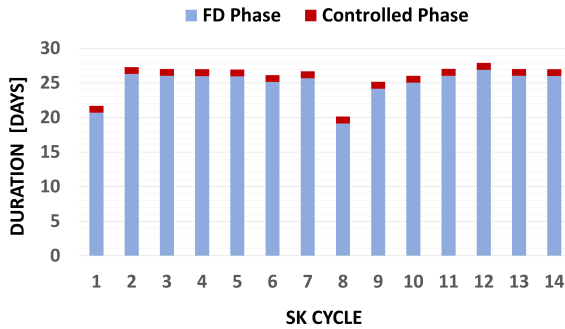


Figure 3: SK Cycles Duration in a Year

The control trajectories are optimized through the minimization of two different cost functions  $J$  over the thrust arc duration  $[t_i, t_f]$ . The EOP minimizes the performance index

$$J = \frac{1}{2} \int_{t_i}^{t_f} \mathbf{u}^T \mathbf{u} dt \quad (9)$$

being  $\mathbf{u}$  the control accelerations vector. The FOP reduce the consumed mass to a minimum

$$J = \frac{T_{max}}{I_{sp}g_0} \int_{t_i}^{t_f} u dt \quad (10)$$

being  $u$  the throttle ranging from 0 to 1,  $I_{sp}$  the specific impulse,  $T_{max}$  the maximum available thrust and  $g_0$  the Earth's gravity acceleration.

#### 3.1. EOP

The state dynamics can be rewritten as:

$$\dot{\mathbf{x}} = f(\mathbf{x}, \mathbf{u}, t) = \tilde{f}(\mathbf{x}, t) + \mathbf{B}(\mathbf{x})\mathbf{u} \quad (11)$$

where  $\tilde{f}(\mathbf{x}, t)$  expresses the dynamics that does not depend on the control and  $\mathbf{B}(\mathbf{x})$  is the input

matrix related to the external commands. The Pontryagin Maximum Principle and the calculus of variations give the expression of  $\mathbf{u}$  with respect to the costate:

$$\mathbf{u} = -\mathbf{B}^T \mathbf{l} \quad (12)$$

and the EOP final TPBVP:

$$\begin{cases} \dot{\mathbf{x}} = \tilde{f}(\mathbf{x}, t) - \mathbf{B}\mathbf{B}^T \mathbf{l} \\ \dot{\mathbf{l}} = -\left(\frac{\partial f(\mathbf{x}, \mathbf{l}, t)}{\partial \mathbf{x}}\right)^T \mathbf{l} \end{cases} \quad (13)$$

Subject to:  $\mathbf{x}(t_i) = \mathbf{x}_{C_i}$  and  $\mathbf{x}(t_f) = \mathbf{x}_T$ . In the EOP case, the SK slot is viewed as a neighbourhood of the nominal satellite location  $\mathbf{x}_n$  (Figure 4). This avoids to compute a reference path, since the considered baseline is the desired SK point, and enables to treat time dependent and time invariant perturbations separately.

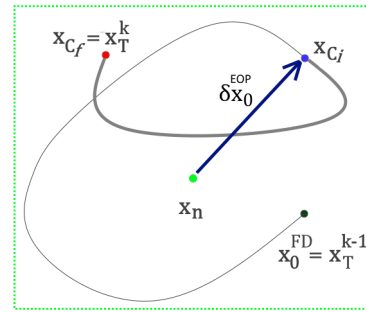


Figure 4: General EOP Solution Design in the Neighbourhood of  $\mathbf{x}_n$

At a control cycle  $k$ , the FD phase starts from the previous loop target  $\mathbf{x}_T^{k-1}$ ; when it ends, the engines are switched on ( $\mathbf{x}_{C_i}$ ), targeting the new objective  $\mathbf{x}_T^k$ . The optimal law  $\delta \mathbf{l}_0$  is obtained with DA as in 8, evaluating the EOP TPBVP polynomial map in the initial perturbation  $\delta \mathbf{x}_0$  and enforcing the final target imposing  $\delta \mathbf{x}_f$  as the inverse of the constant part of the map:  $C = [\mathbf{x}_f] - \mathbf{x}_T$ .

#### 3.2. FOP

The FOP solution is found taking the EOP results as initial guess and leads to a different shape of the control profile. While the EOP is characterized by a continuous action, the FOP generates a *bang-bang* thrust made of a switching sequence between 'ON' ( $u = 1$ ) and 'OFF' ( $u = 0$ ) modes. This commutations ( $t_s$ ) pattern is computed numerically. DA is then used

to build up a robust control trajectory capable of counteracting potential uncertainties or additional perturbations with respect to the reference, as already developed in [3].

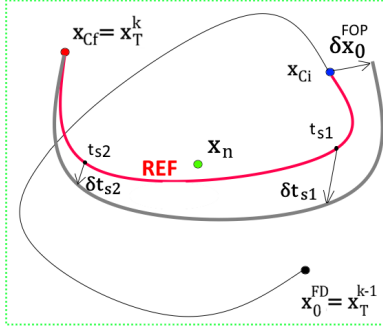


Figure 5: General FOP Solution Design in the Neighbourhood of the Reference Trajectory

The FOP TPBVP assumes the shape:

$$\begin{cases} \dot{\mathbf{x}} = \tilde{f}(\mathbf{x}, t) + \frac{T_{max}}{m} u \mathbf{B} \hat{\alpha} \\ \dot{m} = -\frac{T_{max}}{I_{sp}g_0} u \\ \dot{\mathbf{l}} = -\left(\frac{\partial f(\mathbf{x}, \mathbf{l}, t)}{\partial \mathbf{x}}\right)^T \mathbf{l} \\ \dot{l}_m = -\frac{T_{max} u}{m^2} |\mathbf{l}_v| \end{cases} \quad (14)$$

Subject to:  $\mathbf{x}(t_i) = \mathbf{x}_{Ci}$ ,  $m(t_i) = m_0$ ,  $\mathbf{x}(t_f) = \mathbf{x}_T$  and  $l_m(t_f) = 0$ . Here,  $m$  is the mass of the spacecraft,  $\alpha$  is the direction of the control,  $\mathbf{l}_v$  and  $l_m$  are the velocity and the mass costates respectively. The switching sequence is determined by the sign of the switching function  $\rho$ :  $u = 0$  when  $\rho > 0$ ;  $u = 1$  when  $\rho < 0$ . With

$$\rho = 1 - \frac{I_{sp}g_0}{m} |\mathbf{l}_v| - l_m \quad (15)$$

Solving the FOP is cumbersome, due to its high sensitivity on initial conditions. The transformation from continuous thrust to bang-bang one is reached through the continuation method applied in [3] and consisting in approximating  $u$  as a  $C^\infty$  function as:

$$u = \frac{1}{1 + e^{p\rho}} \quad (16)$$

where  $p$  is a continuation parameter starting from 1 and then increased until the ON-OFF shape appears. Once the numerical baseline is computed, DA is demonstrated to be more powerful than the iterative algorithm for a robust correction of initial displaced conditions.

## 4. Results

The simulations are conducted on a test satellite, whose main parameters are collected in Table 1, and for a SK window made of  $0.1^\circ$  angular bands.

$m_0[kg]$	$A_s[m^2]$	$\beta$	$I_{sp}[s]$	$T[N]$	$l_s[^\circ]$
3000	100	0.5	3800	0.33	$60E$

Table 1: Test Satellite Properties:  $A_s$  reflectivity area;  $\beta$  reflection coefficient;  $T$  max thrust

The findings are computed using the Python interface of the Differential Algebra Computational Toolbox (DACE), on an Intel Core i7-1065G7 1.50 GHz, running Windows 11 Home 64 bit, 16 GB RAM.

### 4.1. EOP Results

In the EOP case the SK control can be directly found by the evaluation of onboard loaded polynomials, reducing the effort to a minimum and satisfying the constraints. In light of the SK strategy adopted, the problem is successfully solved when the final optimized targets are matched with a sufficient precision. The linearized (1<sup>st</sup> order) solution is totally inaccurate and consequently unable to maintain the spacecraft inside its assigned region, as highlighted by Figure 6.

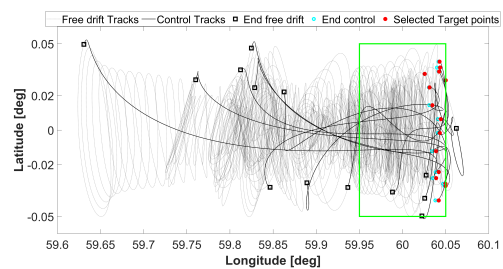


Figure 6: SK Box in a Year. 1<sup>st</sup> order Solution

A 2<sup>nd</sup> order solution is enough to satisfy the SK requirements and obtain almost the same result provided by a numerical single shooting technique. Despite the lack of path constraints causes an eastward violation of the slot during the powered phases, Figure 7 shows high accuracy during the whole SK period. However, since the quadratic DA maps shall be computed every cycle, this approach involves a computational burden of 28.86s in a year, which is slightly

higher than the one required by a shooting algorithm (24.09s).

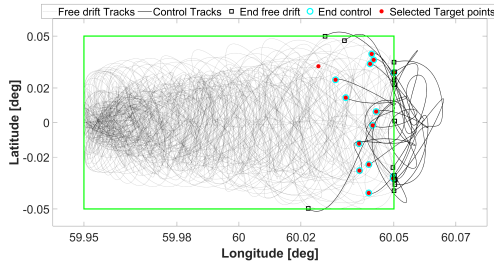


Figure 7: SK Box in a Year. 2<sup>nd</sup> order Solution

Anyway, this is not a complete disadvantage considering that the numerical solution must be run every time a displacement occurs, which is not the case if the control is achieved evaluating a polynomial that expresses the dependence of the final conditions on every possible initial perturbation at that specific cycle. An important reduction of the computational effort (12.22s) is reached separating the autonomous (time invariant) dynamics from the non-autonomous one. This makes it possible to build up a control law evaluating, at every cycle, the same 4<sup>th</sup> order autonomous polynomial and then correcting it with the complete linear (1<sup>st</sup> order) solution. As presented in Figure 8, an interesting output is given by this approach, merging the computational speed of linearized methods and the precision of high order ones. A small violation of the slot occurs both eastwards and westwards but it is limited in time and magnitude. It can be also diminished by decreasing the control duration or by shrinking the target searching box, abandoning the global optimality of the solution.

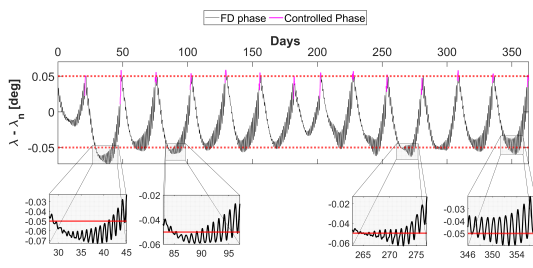


Figure 8:  $\lambda$  in a Year. 4<sup>th</sup> order Autonomous expansion and Linear Correction

There is no criticality on the latitude (Figure 9), well bounded by the assigned constraints, and on the radius, oscillating 10 km around the GEO one (42165 km). Despite a quite high value of

the maximum thrust needed (0.3236 N), a competitive annual  $\Delta v$  of 72.787 m/s is granted.

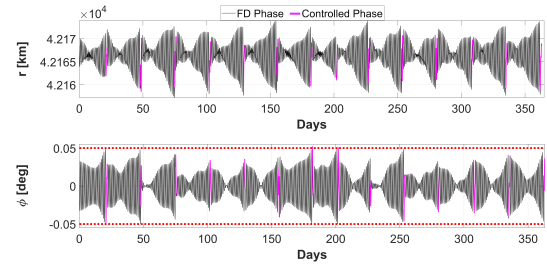


Figure 9:  $r$  and  $\phi$  in a Year. 4<sup>th</sup> order Autonomous expansion and Linear Correction

## 4.2. FOP

In the FOP a robust correction can be obtained around a loaded reference by the onboard expansion of DA quadratic polynomials about it. The EOP one-year consumption is reducible with the FOP bang-bang thrust profile. The numerical FOP reference given by a single shooting approach, initialized by the EOP control law and sequentially solved with the continuation method previously presented, provides a  $\Delta v$  drop to 60.846 m/s, corresponding to only 4.89 kg of burnt gas in a whole year. Due to the high complexity of the problem, an expansion of such a kind takes 41.178s per cycle. This is clearly not convenient when dealing with a displacement in the initial conditions. If the reference is loaded onboard, it is possible to expand a DA polynomial about it for a robust and quick correction counteracting any disturbance. A 2<sup>nd</sup> order DA map of the FOP is available in only 15.044s. When a perturbation occurs, it is able to generate new bang-bang optimal control profiles avoiding to rely on the heavy numerical solution.

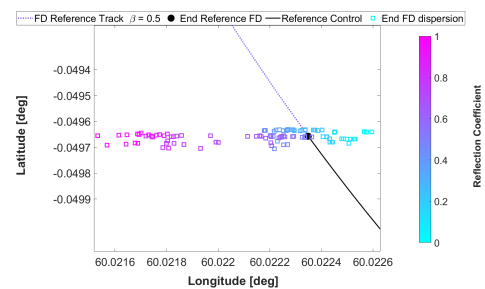


Figure 10: End of FD trajectories. Dispersion due to different  $\beta$

For the first cycle only, a set of 100 initial dis-

placements are considered due to the variation of the reflection coefficient  $\beta$  from 0 (total absorption) to 1 (total reflection). The dispersion at  $\mathbf{x}_{Ci}$  is represented in Figure 10.

The final target is matched by every trajectory by a new set of optimal control profiles depending on  $\beta$ , as in Figure 11.

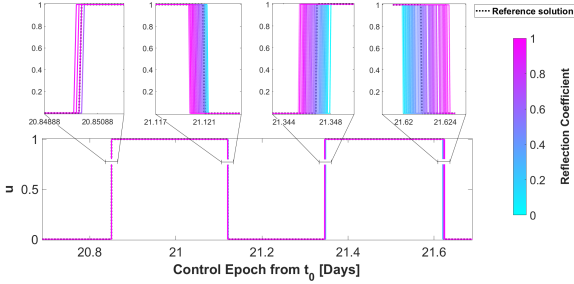


Figure 11:  $u$  Profile Variation

The final dispersion is reduced a lot and the following FD phase remains inside the SK box, as desired (Figure 12). The higher the precision of the control action, the lower the final dispersion. If the accuracy is high enough, the next FD phase trajectories starting from each final control state will collapse into a single path.

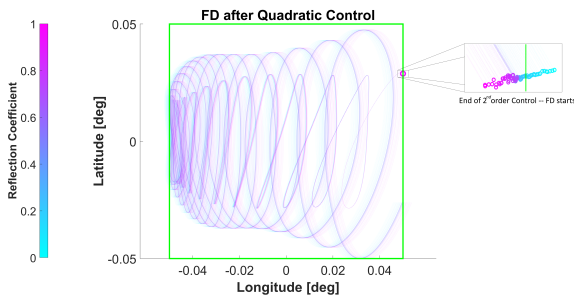


Figure 12: Free-Drift tracks after 2<sup>nd</sup> Order Control

This clearly does not happen if an imprecise linear approach is used (Figure 13).

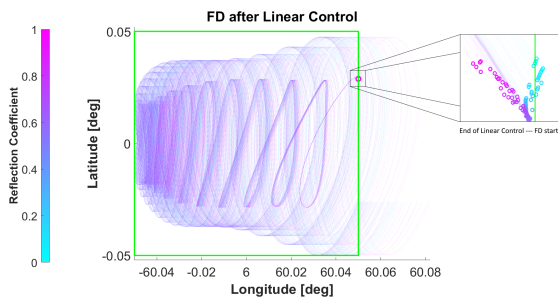


Figure 13: Free-Drift tracks after 1<sup>st</sup> Order Control

## 5. Conclusions

Although a simplified problem is taken into account, its relevant findings suggest further investigations. The power of this method is demonstrated since it grants: an increased precision compared to linearized control; a low computational burden as against numerical techniques; the opportunity to build up a quick and robust controlling action from onboard DA maps; a low overall annual consumption. Future developments could consider to: add path constraints along the powered phases; reduce the maximum value of the thrust needed; consider particular engines configurations and bounds on firing duration and direction; involve the attitude dynamics e.g. adding pointing requirements.

## References

- [1] C. Gazzino, D. Arzeliera, L. Cerri, D. Losa, C. Louembet, and C. Pittet. A three-step decomposition method for solving the minimum-fuel geostationary station keeping of satellites equipped with electric propulsion. *Acta Astronautica 158*: 12-22, 2019.
- [2] P. Di Lizia, R. Armellin, F. Bernelli-Zazzera, and M. Berz. High order optimal control of space trajectories with uncertain boundary conditions. *Acta Astronautica 93*: 217-229, 2014.
- [3] P. Di Lizia, R. Armellin, A. Morselli, and F. Bernelli-Zazzera. High order optimal feedback control of space trajectories with bounded control. *Acta Astronautica 94, Issue 1*: 383-394, 2014.
- [4] P. Di Lizia, R. Armellin, F. Topputo, M. Lavagna, F. Bernelli-Zazzera, and M. Berz. High-order optimal station keeping of geostationary satellites. In *New Trends in Astrodynamics and Applications VI*, 2011.
- [5] A.A. Sukhanov and A.F.B.A. Prado. On one approach to the optimization of low-thrust station keeping manoeuvres. *Advances in Space Research 50*: 1478-1488, 2012.